HHS Public Access

Author manuscript

Hepatology. Author manuscript; available in PMC 2023 February 01.

Published in final edited form as:

Hepatology. 2022 February ; 75(2): 353–368. doi:10.1002/hep.32140.

DUCTULAR REACTION PROMOTES INTRAHEPATIC ANGIOGENESIS VIA SLIT2-ROBO1 SIGNALING

Mar Coll[1,2,3,+,*], **Silvia Ariño**[1,+], **Celia Mártinez-Sánchez**[1], **Ester Garcia-Pras**[1,3], **Javier Gallego**[1,3], **Anna Moles**[4,5], **Beatriz Aguilar-Bravo**[1], **Delia Blaya**[1], **Julia Vallverdú**[1], **Teresa Rubio-Tomás**[1], **Juan Jose Lozano**[3], **Elisa Pose**[1,3,5], **Isabel Graupera**[1,2,3,5], **Andrea Fernández-Vidal**[6], **Albert Pol**[6,7,8], **Ramón Bataller**[9], **Jian-Guo Geng**[10], **Pere Ginès**[1,2,3,5], **Mercedes Fernandez**[2,3], **Pau Sancho-Bru**[1,2,3,*]

[1]Institut d'Investigacions Biomèdiques August Pi i Sunyer (IDIBAPS), Barcelona, Catalonia, Spain.

[2]Medicine department, Faculty of Medicine, University of Barcelona, Barcelona, Catalonia, Spain.

[3]Centro de Investigación Biomédica en Red de Enfermedades Hepáticas y Digestivas (CIBERehd), Barcelona, Catalonia, Spain.

[4]Cell Death and Proliferation, Institute of Biomedical Research of Barcelona, Spanish National Research Council, Barcelona, Catalonia, Spain.

[5]Liver Unit, Hospital Clínic, Barcelona, Catalonia, Spain.

[6]Cell compartments and Signaling Group, Institut d'Investigacions Biomèdiques August Pi i Sunyer (IDIBAPS), Barcelona, Catalonia, Spain.

[7]Department of Biomedical Sciences, Faculty of Medicine, University of Barcelona, Barcelona, Catalonia, Spain.

[8]Institució Catalana de Recerca i Estudis Avançats (ICREA), Barcelona, Catalonia, Spain.

[9]Pittsburgh Liver Research Center, University of Pittsburgh Medical Center, Pittsburgh, Pennsylvania, USA.

[10]Department of Biologic and Material Sciences, University of Michigan School of Dentistry, Ann Arbor, Michigan, USA

[*]Corresponding author: **Correspondence to**: Mar Coll, PhD, Institut d'Investigacions Biomèdiques August Pi i Sunyer (IDIBAPS), Rosselló, 149-153, 08036 Barcelona, Spain, mdcoll@clinic.cat, Tel. +34 932275400 Ext. 4535, Pau Sancho Bru, PhD, Institut d'Investigacions Biomèdiques August Pi i Sunyer (IDIBAPS), Rosselló, 149-153, 08036 Barcelona, Spain, psancho@clinic.cat, Tel. +34 932275400 Ext. 3371.

[+]These authors contributed equally to this work

AUTHOR CONTRIBUTIONS

M.C participated in the design of this study, performed experiments and drafted the manuscript; S.A participated in all the experiments and critically reviewed the manuscript; E.G-P and J.G performed angiogenesis *in vitro* assays; C.M-S performed data analysis. B.A-B participated in liver organoids generation; D.B, J.V and T.R-T helped with the maintenance and genotyping of the ROBO1/2$^{+/-}$ mouse colony. J.L performed bioinformatics analysis; E.P and I.G recruited the patients and critically reviewed the manuscript; A.F-V performed the hepatic hepatectomy surgeries; A.P contribute to the critical review of the manuscript; R.B provided the ARLD sequencing dataset and critically reviewed the manuscript; J.GG provided the ROBO1/2$^{+/-}$ mice and critically reviewed the manuscript; M-F and P.G interpreted data and contributed to the critical review of the manuscript, and P.S-B conceived and designed the study, critically reviewed the manuscript and supervised the study.

CONFLICT OF INTEREST: Nothing to declare.

Abstract

Ductular reaction (DR) expands in chronic liver diseases and correlates with disease severity. Besides its potential role in liver regeneration, DR plays a role in wound-healing response of the liver promoting periductular fibrosis and inflammatory cell recruitment. However, there is no information regarding its role in intrahepatic angiogenesis. In the current study we investigated the potential contribution of DR cells to hepatic vascular remodeling during chronic liver disease. In mouse models of liver injury, DR cells express genes involved in angiogenesis. Among angiogenesis-related genes, the expression of Slit2 and its receptor Robo1 were localized in DR cells and neoangiogenic vessels, respectively. The angiogenic role of the Slit2-Robo1 pathway in chronic liver disease was confirmed in ROBO1/2$^{-/+}$ mice treated with DDC, which displayed reduced intrahepatic neovascular density compared to wild-type mice. However, ROBO1/2 deficiency did not affect angiogenesis in partial hepatectomy. In patients with advanced alcoholic disease, angiogenesis was associated with DR, and upregulation of SLIT2-ROBO1 correlated with DR and disease severity. *In vitro*, human liver-derived organoids produced SLIT2 and induced tube formation of endothelial cells. Overall, our data indicate that DR expansion promotes angiogenesis through the Slit2-Robo1 pathway and recognize DR cells as key players in liver wound-healing response.

Keywords

Alcoholic liver disease; alcoholic hepatitis; Slit2; Robo1; ductular reaction; progenitor cells; organoids

INTRODUCTION

Chronic liver injury drives a wound-healing response in order to maintain liver function and hepatic structural properties. Wound-healing response activates well-coordinated repair mechanisms including hepatocyte proliferation, extracellular matrix turnover and angiogenesis, which induces new blood vessel formation and vascular system remodeling. In this context, ductular reaction (DR) expands as a regenerative response of the liver, sustaining biliary compartment remodeling. DR cells are a heterogeneous population of biliary cells ranging from reactive cholangiocytes to immature liver progenitor cells. The potential of the biliary compartment to contribute to biliary and parenchymal regeneration has been a focus of intense investigation in the field of liver disease (1–5). However, few studies have assessed the interaction of DR cells with their surrounding environment and their role in the wound-healing response of the liver.

Patients with underlying alcohol-related liver disease (ARLD) and heavy alcohol intake can develop episode(s) of alcohol-related hepatitis (AH), which is an acute-on-chronic condition associated with poor short-term prognosis. AH is characterized by inflammatory infiltration, fibrosis, hepatocellular damage and the expansion of DR, which has been associated with disease severity and short-term mortality (6,7). We have recently described that DR cells exhibit a pro-inflammatory profile in AH, increasing liver inflammation and participating in neutrophil chemotaxis (8).

SLIT ligands were first described as secreted chemorepellents of growing axons and migrating neurons that act through Roundabout (Robo) receptors. In recent years, it has been described that guidance cues, which are responsible for neuronal development, have a crucial role in vessel formation (9–11). Among the three SLIT proteins, SLIT2 has emerged as a pro-angiogenic factor by inducing sprouting of new vessel formation in angiogenic tissues. SLIT2 can both positively and negatively modulate angiogenesis by binding to ROBO1 or ROBO4, respectively (12–14). A study on skin and retina showed that Slit2 binding to Robo4 negatively regulates new vessel formation by counteracting vascular endothelial growth factor (VEGF)-mediated angiogenesis (15). The potent pro-angiogenic role of Slit2 has been described mainly in cancer and ischemic diseases (16–19), in which secreted Slit2 by solid tumors binds to Robo1, expressed in vascular endothelial cells, promoting angiogenesis. Conversely, tumor growth can be inhibited by blocking Robo1 activity (13,20). There are few studies assessing the role of the Slit2-Robo1 axis in liver diseases. In this regard, the Slit2-Robo1 pathway was found to be over-expressed in liver cancer and expression of Slit2 and Robo1 was enhanced in fibrotic liver, promoting liver fibrogenesis through hepatic stellate cell activation (21). However, it remains unknown whether the Slit2-Robo1 pathway exerts a pro-angiogenic role in liver regeneration and chronic liver injury.

In this study we hypothesized that DR cells participate in liver tissue remodeling in ARLD. In order to identify pathways in which DR cells are involved, we analyzed the transcriptome of DR cells in a mouse model of chronic liver injury. We identified that liver angiogenesis is a significantly enriched biological process related to DR cells. Additionally, we investigated the role of the Slit2-Robo1 pathway in intrahepatic angiogenesis. The results of our study indicate that DR cells promote liver angiogenesis and that the Slit2-Robo1 pathway is a mechanism underlying this fundamental repair process.

METHODS

Human biopsies and samples

Liver tissue samples were obtained from fragments of non-tumoral cirrhotic liver tissue surrounding colon metastasis collected at the time of liver resection or from explants from liver transplantation due to ARLD, NASH and HCV. The study was approved by the Ethics Committee of the Hospital Clinic of Barcelona and all patients included in this study provided written informed consent.

Patient cohorts

ARLD cohort: Patients with AH and MELD greater than or equal to 21 (n=11), patients with AH and MELD less than 21 (n=18), patients with compensated cirrhosis (n=9) and healthy individuals (n=10).

Chronic liver disease cohort: Patients with AH and MELD greater than or equal to 21 (n=11), patients with AH and MELD less than 21 (n=18), patients with compensated cirrhosis (n=9), patients with ARLD and criteria of steatohepatitis (n=12), patients with NAFLD (n=10), non-cirrhotic HCV (n=10) and healthy individuals (n=10).

The baseline characteristics at the time of liver biopsy of the patients included in the ARLD and chronic liver disease cohorts are described in (23). Moreover, raw sequencing data are available in the Database of Genotypes and Phenotypes (dbGAP) of the National Center for Biotechnology Information phs001807.v1.p1.

AH cohort: Patients with AH (n=29). Patient characteristics are detailed in Supplementary Table 1.

Cirrhotic organoids cohort: Patients with liver cirrhosis (n=5). The etiologies of cirrhosis are described in Supplementary Table 2.

Informed consent in writing was obtained from each patient and the study protocol conformed to the ethical guidelines of the 1975 Declaration of Helsinki as reflected in a priori approval by the appropriate institutional review committee.

Animals

Since complete or partial genetic deletion of *Robo1* is embryonically lethal, we explored the role of Sli2-Robo1 pathway in mice with partial genetic deletion of both *Robo1* and *Robo2* which are viable. ROBO1$^{-/+}$ROBO2$^{-/+}$ (also referred as ROBO1/2$^{-/+}$) mice with BALB/c background were kindly supplied by Dr. Jian-Guo Geng from the University of Michigan. Litter mates of Robo1/2$^{-/+}$ mice were used in all studies. Details on chronic liver injury and regeneration mouse models are described in detail in supplementary information. All animal experiments were approved by the Ethics Committee of Animal Experimentation of the University of Barcelona and were conducted in accordance with the National Institute of Health Guide for the Care and Use of Laboratory Animals.

Gene Ontology Analysis

A microarray analysis of YFP^{+} cells isolated from HNF1βCreER^{YFP} and WT mice receiving the DDC or CDE diet for three weeks (n=3 in all groups) was performed previously (36). In order to assess new biological processes related to DR, we performed a functional analysis using the transcriptomic data generated and deposited in the NCBI Gene Expression Omnibus (GSE51389). A description of the Gene Ontology (GO) analysis (Geneontology.org) performed is detailed in supplementary information.

Liver tissue and organoid analysis

Details on immunostaining of liver tissue and organoids protocol as well as gene expression, western blot and hydroxyproline analysis of liver tissue samples are detailed in supplementary information.

In vitro angiogenesis assay

Growth factor-reduced Matrigel (BD Biosciences, San Jose, CA) was completely thawed at 4°C for 16–24h before conducting the tube formation assay. Liquid Matrigel was added to a previously chilled 24-well plate (300 μL/well). The plate was then incubated 1 hour at 37°C to allow Matrigel solidification. HUVECs(60,000 cells/well) were resuspended in basal medium (DMEM-F12, 1% Glutamax, 1% Hepes and 1% penicillin/streptomycin) or

basal medium with recombinant SLIT2 protein (2ng/mL). To further explore the role of organoid-derived SLIT2 in promoting angiogenesis, we pre-incubated HUVEC cells for 2 hours with or without 10mg/mL of sheep anti-human ROBO1 antibody (R&D Systems) in basal medium. Following, HUVECs were stimulated with conditioned medium with and without αROBO1 antibody (10mg/mL). In all conditions, HUVECs were incubated for 12 hours at 37°C, 5% CO_2. Then, the medium was removed and the endotubes were rinsed with PBS and fixed with 4% paraformaldehyde for 15 minutes. Tubules were visualized by phase-contrast microscopy and 6 images/well at 4X were taken. Tube formation was evaluated by Angiogenesis Analyzer tool (ImageJ software).

Liver organoids generated from cirrhotic liver tissues

Liver organoids were generated from cirrhotic liver tissue samples and cultured following the protocol previously described with minor modifications (8). Briefly, liver tissue was digested using Collagenase XI (Sigma-Aldrich) and Dispase II (ThermoFisher) for 30 minutes at 37°C. After washing and erythrocyte lysis steps, pelleted cells were embedded in basement matrix extract (BME; Amsbio, Abingdon, United Kingdom) and seeded in 24-well plates. Following BME solidification, organoid expansion medium was added. Organoid expansion medium consisted in basal medium [Advanced DMEM/F12 (ThermoFisher), 1% Glutamax (ThermoFisher), 1% Hepes (Life Technologies, Carlsbad, CA) and 1% penicillin-streptomycin (Lonza, Basilea, Switzerland)] supplemented with % N2 and 1% B7 without vitamin A (both from Life Technologies), 1.25 mM N-acetylcysteine, 10 mM nicotinamide and 10 nM gastrin (Sigma-Aldrich), 50 ng/mL epidermal growth factor, 100 ng/mL fibroblast growth factor 10, 25 ng/mL hepatocyte growth factor, 25 ng/mL Noggin and 500 ng/mL Rspo1 (Peprotech, London, United Kingdom), 5 uM A8301, 0.5 uM CHIR99021, 10 uM Forskolin, and 10 uM of Y27632 (Axon Medchem, Groningen, the Netherlands). Y27632 was added only the first 3 days after isolation. The expansion medium was replaced every 2–3 days, and cells were split once a week. At a confluence of 70–80%, organoid expansion medium was replaced by basal medium for 18 hours. Organoid conditioned medium was collected and stored at −80°C until HUVECs tubulogenic assay and ELISA SLIT2 quantification were performed.

Serum SLIT2 detection

SLIT2 serum levels from healthy individuals and AH patients as well as from supernatants of liver organoids generated from cirrhotic patients were evaluated with a specific ELISA kit for SLIT2 (Cusabio Biotech Co., Wuhan, China) following the manufacturer's protocol.

Statistical analysis

Values are expressed as a mean± standard error of the mean (SEM). Statistical differences between groups were analyzed using the Student's t test, two-way ANOVA with Bonferroni correction or the Mann-Whitney *U* test when appropriate with GraphPad Prism 5.0 (San Diego, CA, USA). A $p \leq 0.05$ was considered statistically significant. Correlations between variables were evaluated using Spearman's *rho* or Pearson's *r*, when appropriate.

RESULTS

Mouse ductular reaction cells exhibit enriched expression of genes related to angiogenesis

In order to identify new biological functions associated with DR cells, we evaluated transcriptomic data obtained from biliary cells, isolated as YFP^+ cells by FACS sorting, from $HNF1\beta CreER^{YFP}$ mice. DR cells were isolated from mice fed with a diet enriched in 3, 5-diethoxycarbonyl-1, 4-dihydro-collidin (DDC), a choline-deficient ethionine-supplemented diet (CDE) or with chow diet for 3 weeks and also from control mice. Gene ontology (GO) analysis revealed that the top 5 enriched biological processes associated with DR cells were: inflammatory response (gene ratio: 37/315, p: $1{\cdot}10^{-9}$) followed by regulation of cell adhesion (gene ratio: 31/315, p: $8{\cdot}10^{-9}$), angiogenesis (gene ratio: 25/315, p: $9{\cdot}10^{-8}$), tube morphogenesis (gene ratio: 33/315, p: $3.7{\cdot}10^{-7}$) and blood vessel morphogenesis (gene ratio: 26/315, p: $1.18{\cdot}10^{-6}$) (Figure 1A). Since very little is known regarding the capacity of DR cells to participate in angiogenesis, we decided to focus on this key repair mechanism. In order to investigate the mechanism by which DR contributes to liver angiogenesis, we examined the molecules underlying the GO terms related to angiogenesis (Figure 1B). *Slit2*, a well described pro-angiogenic factor, was the gene included in all the categories. Moreover, *Slit2* was found to be significantly upregulated in YFP^+ cells isolated from the DDC and CDE models compared to those sorted from control mice (FC=2.2, p=0.004 and FC=7.48, p=0.002, respectively) (Figure 1C).

Slit2 is expressed by ductular reaction cells and *Robo1* by vessels in DDC mice

Slit2 acts as a regulator of new vessel formation through interactions with either Robo1 or Robo4 receptors in the context of cancer and ischemic diseases (16–19). In order to assess the role of Slit2 in intrahepatic angiogenesis, we first examined the levels of *Slit2* expression and its receptors in liver tissue from DDC and CDE mouse models. *Slit2* was found to be up-regulated in DDC and CDE compared to control livers (FC= 44.8±4.6 and FC= 8.2±3.3, respectively) at similar levels to the DR markers *Epcam* and *Krt19*. We also observed a significant up-regulation of *Robo1* in both models (FC=3.9±0.15 and FC= 2.25±0.3, respectively), whereas *Robo4* was not found to be differentially expressed (Figure 2A). In order to confirm that the expression of *Slit2* was restricted to DR cells, we analyzed the gene expression levels of *Slit2* in both YFP^+ isolated cells and a hepatocyte fraction from DDC mice using quantitative real-time PCR (qPCR). As shown in Figure 2B, while *Slit2* was found to be significantly enriched in DR cells compared to total liver tissue, no expression was found in the hepatocyte fraction (Figure 2B). As expected, we did not find *Robo1* expression in either of the examined cell fractions. Next, by performing immunohistochemistry in DDC livers, we confirmed that SLIT2 was expressed by the ductular structures (KRT19 positive cells), whereas its receptor ROBO1 was expressed by the endothelial cells comprising the new vessels located near the peri-portal areas (Figure 2C). It is important to note that *Robo1* expression was not detected in endothelial cells of the portal vein or hepatic artery indicating that its expression is specific to the neo-angiogenic endothelial cells. These results indicate that, in a DDC mouse model, DR structures express the pro-angiogenic factor SLIT2, which might interact with ROBO1 receptors expressed by the neo-vessels.

ROBO1/2$^{-/+}$ mice display reduced hepatic angiogenesis compared to wild-type mice in response to DDC-induced injury

In order to determine the functional role of Slit2-Robo1 signaling in the pathogenesis of chronic liver injury, we used Robo1/2 partial knockout mice (ROBO1/2$^{-/+}$) and wild type littermates (WT) with DDC and CDE diets, both involving DR expansion, for 3 and 4 weeks, respectively. Immunohistochemistry of DR key markers such as KRT19 and EPCAM revealed that ROBO1/2$^{-/+}$ mice fed with DDC and CDE did not display a reduction in DR structures compared to WT mice, indicating that Slit2-Robo1 signaling is not directly involved in ductular cell proliferation (Figure 3A and 3B). In line with this result, we did not find significant differences in the hepatic expression of genes related to DR such as *Krt19, Epcam or Sox9* (Supplementary Figure 1A and 2A). In addition, we observed that fibrosis assessed by Sirius Red staining, gene expression of *Acta2*, *Col1a1*, *Mmp2* and *Timp1* and by liver hydroxyproline level determination was not altered in ROBO1/2$^{-/+}$ mice treated with DDC or CDE when compared to WT mice (Figure 3A, 3B, Supplementary Figure 1B and 2B and 3). Indeed, although a pro-fibrogenic role of Slit2-Robo1 signaling has been previously reported in a mouse model of advanced fibrosis based on chronic CCl4 administration, it has been attributed to Slit2 expression by hepatic stellate cells. Interestingly, quantification of immunohistochemistry staining for CD31 showed a marked reduction of vessels surrounding peri-portal areas in ROBO1/2$^{-/+}$ compared to WT mice in both injury models. However, we did not observe a major gene expression reduction of key markers related to angiogenesis (Figure 3, Supplementary Figure 1C and 2C). Moreover, we did not observe any differences in liver enzymes in serum of ROBO1/2$^{-/+}$ fed with DDC or CDE compared to WT (Supplementary Figure 4A and 4B). These results demonstrate that Slit2-Robo1 signaling regulates hepatic angiogenesis in both models of chronic liver disease involving DR expansion.

Slit2-Robo1 signaling does not participate in modulating physiological angiogenesis in response to partial hepatectomy

After partial hepatectomy, angiogenesis and angiocrine growth factors play a key role in the correct regeneration of the liver (22). Since Slit2-Robo1 has a role in regulating hepatic angiogenesis in chronic liver damage, we assessed whether this signaling pathway participates in the regeneration mechanisms of a healthy liver. With this objective, we first performed two thirds partial hepatectomy in C57BL/6J mice. We assessed the hepatic gene expression of *Slit2* and *Robo1* together with DR markers (*Epcam, Krt19, Sox9*) at different stages of liver regeneration after partial hepatectomy, considering early (0, 24, 48 and 24 hours) and late time points (day 7 and 28) after surgery. Interestingly, we found increased *Slit2* expression at 48 hours, 72 hours and day 7 after partial hepatectomy compared to intact liver at 0 hours. Besides, liver expression of *Robo1* was significantly up-regulated at 72h after the surgery (Figure 4A). Next, to assess the potential role of Slit2-Robo1 signaling in physiologic angiogenesis, we performed partial hepatectomy in ROBO1/2 $^{-/+}$ mice and WT littermates. We evaluated liver regeneration at 48 hours and day 7 after partial hepatectomy. We did not find significant differences in the number of proliferating cells within the parenchyma, assessed by immunohistochemistry of KI67 between ROBO1/2 $^{-/+}$ and WT mice in early (48hours) or late (7 days) time point after surgery (Figure 4B and Supplementary Figure 6B). Likewise, liver regeneration index, calculated as liver weight/

body weight ratio, did not change either (Supplementary Figure 5A and 6A). Regarding liver progenitor cell expansion, we found a down-regulation of *Epcam and Krt19* gene expression in ROBO1/2 $^{-/+}$ mice at early but not at late time points after partial hepatectomy when compared to WT mice. However, we did not see any differences in DR expansion as assessed by immunohistochemistry of KRT19 at 48 and 7 days after surgery (Figure 4B and 4C, Supplementary Figure 5B and 6C) suggesting that liver regeneration is not affected by Robo1 deficiency in partial hepatectomy. To specifically investigate whether angiogenesis was impaired in ROBO1/2$^{-/+}$ mice, we quantified CD31 stained vessels within the liver tissue. We did not observe differences in the formation of new vessels in early or late time points after partial hepatectomy, indicating that Slit2-Robo1 signaling does not significantly contribute to physiological angiogenesis (Figure 4B and 4C). These results suggest that, although there is an activation of Slit2-Robo1 pathway after partial hepatectomy, other mechanisms, possibly mediated by VEGF, are more relevant in driving angiogenesis during hepatic regeneration of healthy liver.

Ductular reaction and the Slit2-Robo1 pathway are associated with ALD progression

DR is a histological key feature of AH and increases along ARLD progression. Given the pro-angiogenic role of SLIT2 in mouse models involving DR expansion, we hypothesized that DR contributes to tissue repair along ARLD progression by promoting angiogenesis via Slit2-Robo1 signaling. In order to assess this hypothesis, we first showed that neo-angiogenesis was taking place near the DR structures in liver tissues from patients with cirrhosis and AH by performing a double immunohistochemistry of VWF and KRT7 (Figure 5A). Next, we examined the levels of *SLIT2* and *ROBO1* expression as well as the gene expression profile of gene sets related to angiogenesis and DR in RNA sequencing data from total liver tissue from a cohort of patients encompassing the whole spectrum of ARLD (23). The patients included in this cohort were grouped according to ARLD stages: severe AH: patients with AH and MELD greater than or equal to 21 (n=11), non-severe AH: patients with AH and MELD less than 21 (n=18), patients with compensated cirrhosis (n=9) and healthy individuals (n=10). Interestingly, the expression profile of the angiogenesis gene set markedly increased with ARLD progression, suggesting that intrahepatic angiogenesis is a relevant regeneration mechanism underlying ARLD. As expected, the DR gene signature increased in ARLD progression, and we found that it followed a similar gene expression pattern as angiogenesis. In addition, *SLIT2* and *ROBO1* expression displayed a similar trend to DR and angiogenesis sets, showing significant up-regulation in severe compared to non-severe AH (Figure 5B). Next, we sought to determine if DR and angiogenesis were linked biological processes in patients with chronic liver diseases of different etiologies. For this analysis we included a group of patients with non-advanced chronic liver disease with the following etiologies: ARLD with histologic criteria of steatohepatitis (n=12), non-alcoholic fatty liver disease (NAFLD) (n=10) and non-cirrhotic hepatitis C virus (HCV)-infected patients (n=10). The hepatic expression of DR markers (*KRT7* and *KRT19*) strongly correlated with the expression of angiogenesis markers such as *PECAM* and *VWF* (Figure 5C) as well as with *SLIT2* and its receptor *ROBO1* (Figure 5D). This result suggests that DR expansion and angiogenesis are activated not only along ARLD progression but also in chronic liver diseases of other etiologies. Moreover, our findings indicate that the Slit2-Robo1 pathway is associated with fundamental repair processes in chronic liver disease

such as DR and angiogenesis. In addition, the expression of the angiogenic signaling factor *VEGFA* and the receptors *KDR* and *FLT1* did not correlate with the hepatic expression of DR markers (Supplementary Figure 7), suggesting that in chronic liver disease, DR-mediated angiogenesis may not be related to VEGFA signaling.

The Slit2-Robo1 pathway is enhanced in patients with alcoholic hepatitis

To confirm the association of DR with the Slit2-Robo1 pathway we evaluated the hepatic expression of *SLIT2* and its receptor *ROBO1* in a cohort of AH patients (n=29) and healthy individuals (n=5). The characteristics of the patients are described in Supplementary Table 1. As shown in Figure 6, *SLIT2* and *ROBO1* expression was increased in AH patients compared to controls (FC=3.4±0.4, and FC=2.35±019, respectively). As expected, the hepatic expression of *SLIT2* significantly correlated with the expression of its receptor *ROBO1*. Interestingly, in the same cohort of AH patients, *SLIT2* expression strongly correlated with the hepatic expression of *KRT7*, suggesting that DR cells are a cell source of SLIT2 in AH patients (Figure 6A). Next, we investigated the serum levels of SLIT2 in a subset of patients with AH (n=16) and healthy individuals (n=6). As shown in Figure 6B, we observed that circulating SLIT2 levels were significantly increased in AH patients compared to healthy individuals (9.8±0.9 vs. 3.4±1.1 ng/mL). Additionally, circulating levels of SLIT2 positively correlated with serum levels of aspartate aminotransferase (AST) and alkaline phosphatase (AP), suggesting that SLIT2 increases together with liver injury in AH.

Ductular reaction cells from cirrhotic livers secrete SLIT2 and induce tubulogenesis

We recently reported that liver organoids derived from cirrhotic liver tissue mimic DR cells and represent a relevant *in vitro* model to study DR (8). In order to confirm that human DR cells secrete SLIT2, we generated liver biliary organoids from patients with cirrhosis of different etiologies (non-alcoholic steatohepatitis (NASH), n=1; ARLD, n=2 and HCV, n=2). The cirrhotic tissues used to generate organoids expressed higher levels of SLIT2 and ROBO1 proteins compared to control livers (Figure 6C). We also confirmed the presence of DR in all the cirrhotic tissue samples examined by KRT7 immunohistochemistry (Supplementary Figure 8A). As expected, we detected the SLIT2 protein in all the supernatants of the organoids generated (17±2.8 ng/ml) (Supplementary Table 2 and Supplementary Figure 8B), and we observed SLIT2 expression by immunofluorescence in the liver organoid (Supplementary Figure 8C). Next, with the purpose of demonstrating the pro-angiogenic potential of DR cells, we performed a tubulogenic assay by exposing human umbilical vein endothelial cells (HUVECs) to conditioned medium derived from cirrhotic liver organoids (n=3). As a positive control, we incubated HUVECs with recombinant SLIT2 protein (2ng/mL). Compared to the basal medium, liver organoid conditioned medium significantly increased angiogenesis, as assessed by the quantification of the number of junctions formed by HUVECs. To further demonstrate that Slit2 secreted by DR cells mediate angiogenesis, we treated HUVECs with conditioned medium containing αROBO1 blocking antibody. Interestingly, we observed that the pro-angiogenic ability of DR cells was significantly attenuated after ROBO1 blockade (Figure 6D and Supplementary Figure 8D). Altogether, these results suggest that DR cells release the pro-angiogenic factor SLIT2, thus contributing to angiogenesis.

DISCUSSION

In this study we show that DR may promote intrahepatic angiogenesis in chronic liver diseases. We show that DR structures express SLIT2 whereas its receptor ROBO1 is expressed by endothelial cells of small vessels. We describe that the Slit2-Robo1 pathway regulates intrahepatic angiogenesis in chronic liver injury but not in physiological liver regeneration induced by loss of liver cell mass. Moreover, we describe that intrahepatic angiogenesis and DR expansion are concomitant mechanisms taking place along ARLD progression. With the use of a human *in vitro* model of DR cells, we demonstrate the capacity of DR cells to produce SLIT2 and induce angiogenesis. Collectively, these data indicate that DR cells trigger intrahepatic liver angiogenesis through the Slit2-Robo1 pathway.

Under chronic liver damage, the intrahepatic vascular bed undergoes a critical structural modification by enhancing the number of sinusoidal vessels and producing shunts connecting central and portal venules to reduce sinusoidal vascular resistance (24). In the present study, we show that intrahepatic angiogenesis increases with disease progression, indicating that liver angiogenesis behaves as a dynamic process following the same pattern as other repair mechanisms such as fibrogenesis. In this regard, previous studies have evaluated the therapeutic potential of preventing hepatic angiogenesis as a strategy to reduce disease progression. However, the beneficial effects of the administration of anti-angiogenic drugs in animal models of chronic liver injury is still controversial (25,26). In fact, angiogenesis is a fundamental mechanism underlying liver injury repair and regeneration, and therefore, it may play a beneficial role in the wound-healing response to injury. To understand to what extent the intrahepatic angiogenesis is contributing to disease progression and tissue healing in chronic liver diseases is a very important aspect with clinical implications that should be directly investigated.

DR cells are known to play a role in liver fibrosis and inflammation (8,27,28). However, there is a lack of information regarding the potential of DR in promoting angiogenesis. In order to elucidate whether DR participates in angiogenesis, we performed a GO analysis with the transcriptomic data generated from DR cells isolated from mice subjected to chronic injury involving DR expansion (3 weeks of DDC and CDE diets). Interestingly, angiogenesis was found to be one of the most enriched biological processes associated with mouse DR. In humans, in a large cohort encompassing the whole spectrum of ARLD, we confirmed that DR expansion correlates with intrahepatic expression of angiogenic factors and markers, and that both mechanisms paralleled disease progression.

Intrahepatic angiogenesis takes place under the physiological context of liver regeneration and under pathological conditions (29,30). To investigate whether the Slit2-Robo1 pathway promotes angiogenesis in these contexts, we used chronic injury (3 and 4 weeks of DDC and CDE diets, respectively) and liver regeneration (partial hepatectomy) models in mice with a partial deletion of *Robo1* and *Robo2* genes, since complete deletion of *Robo1* is embryonically lethal. Interestingly, we show that the Slit2-Robo1 pathway promotes liver angiogenesis in response to chronic injury but does not contribute to remodeling the vascular bed during liver regeneration after partial hepatectomy. These data indicate that angiogenesis

driven by Slit2-Robo1 pathway may be taking place only in the context of chronic liver injury where ductular reaction expansion is present, but not in a regenerative response in a healthy liver, where there is no involvement of the ductular reaction. These results suggest that Slit2-Robo1 pathway may be a potential target to enhance liver wound-healing in chronic liver disease. In fact, it is known that Slit2-Robo1 signaling participates in promoting angiogenesis in several pathological contexts such as retinopathy (31), ischemia (18) or endometriosis (32). In addition, Slit2 expression in solid tumors promotes tumor-induced angiogenesis by acting through Robo1 expressed in vascular endothelial cells (13). Further studies are needed to elucidate whether intrahepatic Slit2 contributes to angiogenesis in other pathological liver settings such as tumor angiogenesis.

Little is known regarding the mechanisms that trigger pathological intrahepatic angiogenesis. To date, the main cell type inducing liver angiogenesis in a pathological setting is liver endothelial sinusoidal cells, although hepatic stellate cells also directly contribute to new vessel formation by producing pro-angiogenic factors such as VEGF, platelet-derived growth factor (PDGF) and angiopoietin-1 (ANG-1) or in a paracrine manner by activating liver sinusoidal endothelial cells (33,34). Our study focused on intrahepatic angiogenesis underlying chronic liver diseases with DR expansion such as ARLD. In this context, we showed that the neo-angiogenesis, which is histologically visualized as small vessels with varying diameter and positive staining for VWF or CD31, takes place near the proliferative ductular structures. To confirm the angiogenic role of DR cells, we generated biliary 3D organoids derived from cirrhotic liver tissue, which have shown to retain the phenotypic and transcriptomic features of DR cells mimicking *in vitro* DR (8). In this regard, we demonstrate that all DR organoids generated from different etiologies (ARLD and NASH), secrete SLIT2 and induce HUVECs tube formation.

Interestingly, serum SLIT2 levels are increased and correlate with the severity of liver injury in AH patients, the most severe form of ARLD that is characterized by extensive DR. These results are in agreement with previous data showing increased circulating levels of SLIT2 in patients with fibrosis (21). In addition, activated hepatic stellate cells produce and are also targets of SLIT2, contributing to fibrogenesis. These results indicate that DR cells are not the only cell source of Slit2 in chronic liver disease and suggest that Slit2 secreted by DR cells could contribute to wound-healing repair not only by inducing angiogenesis but also by targeting hepatic stellate cells and promoting fibrogenesis.

Although we have shown that DR cells promote angiogenesis via the Slit2-Robo1 pathway, DR may also produce other pro-angiogenic factors. Histologically, it has been shown that liver progenitor cells derived from primary biliary cholangitis patients express VEGFA and VEGFC at a protein level (35). However, in the ARLD cohort, we did not find a correlation between the hepatic expression of *VEGFA* and the expression pattern of genes related to DR, suggesting that intrahepatic expression of *VEGFA* does not occur in parallel with DR expansion.

DR cells have the potential to contribute to liver regeneration by giving rise to new hepatocytes when their replication capacity is hampered. In this study, we provide evidence to support that DR cells contribute to tissue remodeling by promoting angiogenesis.

In addition, we have recently reported that in chronic liver damage, DR cells produce chemoattractant agents to induce neutrophil recruitment that might also participate in liver tissue repair (8). Taken together, these results suggest that DR has a major role in liver wound-healing, driving fundamental repair mechanisms.

Overall, this report provides evidence that DR cells mediate intrahepatic angiogenesis via the Slit2-Robo1 pathway and recognizes DR cells as important contributors to wound-healing repair processes in chronic liver disease.

Supplementary Material

Refer to Web version on PubMed Central for supplementary material.

ACKNOWLEDGMENTS

This work was performed in the Centre Esther Koplowitz. We thank Dr. Jian-Guo Gen from the University of Michigan for kindly providing the ROBO1$^{-/+}$ROBO2$^{-/+}$ mice and for his scientific support. The authors thank Cristina Millán for her excellent technical support especially in immunohistochemistry. We are indebted to the Cytomics Unit, Genomics Unit and Biobank core facility of the Institut d'Investigacions Biomèdiques August Pi i Sunyer (IDIBAPS) for technical help

Financial support:

This work has been supported by grants from Fondo de Investigación Sanitaria Carlos III (FIS), co-financed by Fondo Europeo de Desarrollo Regional (FEDER), Unión Europea, "Una manera de hacer Europa" (FIS PI20/00765, PI17/00673 to P.S.-B and FIS 18-PI18/00862 to I.G and M.C), from the NIH National Institute on Alcohol Abuse and Alcoholism grant 1U01AA026972-01 and from AGAUR 2017-SGR-01456 to P.S.-B., and from the European Foundation for Alcohol Research (ERAB) Grant EA1653 to P.S.-B. M.C is funded by Ramon y Cajal program from the Ministerio de Ciencia e Innovación RYC2019-026662-I. P.G. is funded by Agencia de Gestió d'Ajuts Universitaris i de Recerca (AGAUR) 2014 SGR 708, Centro de Investigaciónen Red Enfermedades Hepáticas y Digestivas (CIBERehd) and Institució Catalana de Recerca i Estudis Avançats (ICREA). S.A received a grant from the Ministerio de Educación, Cultura y Deporte, FPU programme (FPU17/04992). B.A.-B. is funded by Instituto de Salud Carlos III, PFIS (FI16/00203).

REFERENCES

1. Huch M, Dorrell C, Boj SF, Van Es JH, Li VSW, Van De Wetering M, et al. In vitro expansion of single Lgr5 + liver stem cells induced by Wnt-driven regeneration. Nature. 2013 Feb 14;494(7436):247–50. [PubMed: 23354049]
2. Tarlow BD, Finegold MJ, Grompe M. Clonal tracing of Sox9+ liver progenitors in mouse oval cell injury. Hepatology. 2014 Jul 1;60(1):278–89. [PubMed: 24700457]
3. Deng X, Zhang X, Li W, Feng RX, Li L, Yi GR, et al. Chronic Liver Injury Induces Conversion of Biliary Epithelial Cells into Hepatocytes. Cell Stem Cell. 2018 Jul 5;23(1):114–122.e3. [PubMed: 29937200]
4. Malato Y, Naqvi S, Schürmann N, Ng R, Wang B, Zape J, et al. Fate tracing of mature hepatocytes in mouse liver homeostasis and regeneration. J Clin Invest. 2011 Dec 1;121(12):4850–60. [PubMed: 22105172]
5. Raven A, Lu WY, Man TY, Ferreira-Gonzalez S, O'Duibhir E, Dwyer BJ, et al. Cholangiocytes act as facultative liver stem cells during impaired hepatocyte regeneration. Nature. 2017 Jul 20;547(7663):350–4. [PubMed: 28700576]
6. Gao B, Bataller R. Alcoholic liver disease: Pathogenesis and new therapeutic targets. Vol. 141, Gastroenterology. W.B. Saunders; 2011. p. 1572–85. [PubMed: 21920463]
7. Sancho-Bru P, Altamirano J, Rodrigo-Torres D, Coll M, Millán C, José Lozano J, et al. Liver progenitor cell markers correlate with liver damage and predict short-term mortality in patients with alcoholic hepatitis. Hepatology. 2012 Jun 1;55(6):1931–41. [PubMed: 22278680]

8. Aguilar-Bravo B, Rodrigo-Torres D, Ariño S, Coll M, Pose E, Blaya D, et al. Ductular Reaction Cells Display an Inflammatory Profile and Recruit Neutrophils in Alcoholic Hepatitis. Hepatology. 2019 May 12;69(5):2180–95. [PubMed: 30565271]
9. Andrews W, Barber M, Hernadez-Miranda LR, Xian J, Rakic S, Sundaresan V, et al. The role of Slit-Robo signaling in the generation, migration and morphological differentiation of cortical interneurons. Dev Biol. 2008 Jan 15;313(2):648–58. [PubMed: 18054781]
10. Andrews WD, Barber M, Parnavelas JG. Slit-Robo interactions during cortical development. In: Journal of Anatomy. Wiley-Blackwell; 2007. p. 188–98.
11. Ba-Charvet KTN, Brose K, Marillat V, Kidd T, Goodman CS, Tessier-Lavigne M, et al. Slit2-mediated chemorepulsion and collapse of developing forebrain axons. Neuron. 1999 Mar 1;22(3):463–73. [PubMed: 10197527]
12. Suchting S, Heal P, Tahtis K, Stewart LM, Bicknell R. Soluble Robo4 receptor inhibits in vivo angiogenesis and endothelial cell migration. FASEB J. 2005 Jan 14;19(1):121–3. [PubMed: 15486058]
13. Wang B, Xiao Y, Ding BB, Zhang N, Bin Yuan X, Gui L, et al. Induction of tumor angiogenesis by Slit-Robo signaling and inhibition of cancer growth by blocking Robo activity. Cancer Cell. 2003 Jul 1;4(1):19–29. [PubMed: 12892710]
14. Park KW, Morrison CM, Sorensen LK, Jones CA, Rao Y, Bin Chien C, et al. Robo4 is a vascular-specific receptor that inhibits endothelial migration. Dev Biol. 2003 Sep 1;261(1):251–67. [PubMed: 12941633]
15. Jones CA, London NR, Chen H, Park KW, Sauvaget D, Stockton RA, et al. Robo4 stabilizes the vascular network by inhibiting pathologic angiogenesis and endothelial hyperpermeability. Nat Med. 2008 Apr 16;14(4):448–53. [PubMed: 18345009]
16. Alajez NM, Lenarduzzi M, Ito E, Hui ABY, Shi W, Bruce J, et al. miR-218 suppresses nasopharyngeal cancer progression through downregulation of survivin and the SLIT2-ROBO1 pathway. Cancer Res. 2011 Mar 15;71(6):2381–91. [PubMed: 21385904]
17. Chang PH, Hwang-Verslues WW, Chang YC, Chen CC, Hsiao M, Jeng YM, et al. Activation of Robo1 signaling of breast cancer cells by Slit2 from stromal fibroblast restrains tumorigenesis via blocking PI3K/Akt/β-catenin pathway. Cancer Res. 2012 Sep 15;72(18):4652–61. [PubMed: 22826604]
18. Li X, Zheng S, Tan W, Chen H, Li X, Wu J, et al. Slit2 Protects Hearts Against Ischemia-Reperfusion Injury by Inhibiting Inflammatory Responses and Maintaining Myofilament Contractile Properties. Front Physiol. 2020 Mar 27;11:228. [PubMed: 32292352]
19. Chaturvedi S, Yuen DA, Bajwa A, Huang YW, Sokollik C, Huang L, et al. Slit2 prevents neutrophil recruitment and renal ischemia-reperfusion injury. J Am SocNephrol. 2013 Jul 31;24(8):1274–87.
20. Wang L-J, Zhao Y, Han B, Ma Y-G, Zhang J, Yang D-M, et al. Targeting Slit–Roundabout signaling inhibits tumor angiogenesis in chemical-induced squamous cell carcinogenesis. Cancer Sci. 2008 Mar 1;99(3):510–7. [PubMed: 18201275]
21. Chang J, Lan T, Li C, Ji X, Zheng L, Gou H, et al. Activation of Slit2-Robo1 signaling promotes liver fibrosis. J Hepatol. 2015 Dec 1;63(6):1413–20. [PubMed: 26264936]
22. Sen Ding B, Nolan DJ, Butler JM, James D, Babazadeh AO, Rosenwaks Z, et al. Inductive angiocrine signals from sinusoidal endothelium are required for liver regeneration. Nature. 2010 Nov 11;468(7321):310–5. [PubMed: 21068842]
23. Argemi J, Latasa MU, Atkinson SR, Blokhin IO, Massey V, Gue JP, et al. Defective HNF4alpha-dependent gene expression as a driver of hepatocellular failure in alcoholic hepatitis. Nat Commun. 2019 Dec 1;10(1):1–19. [PubMed: 30602773]
24. Iwakiri Y, Shah V, Rockey DC. Vascular pathobiology in chronic liver disease and cirrhosis - Current status and future directions. Vol. 61, Journal of Hepatology. Elsevier B.V.; 2014. p. 912–24. [PubMed: 24911462]
25. Patsenker E, Popov Y, Stickel F, Schneider V, Ledermann M, Sägesser H, et al. Pharmacological inhibition of integrin αvβ3 aggravates experimental liver fibrosis and suppresses hepatic angiogenesis. Hepatology. 2009;50(5):1501–11. [PubMed: 19725105]

26. Mejias M, Garci-Pras E, Tiani C, Miquel R, Bosch J, Fernandez M. Beneficial effects of sorafenib on splanchnic, intrahepatic, and portocollateral circulations in portal hypertensive and cirrhotic rats. Hepatology. 2009;49(4):1245–56. [PubMed: 19137587]
27. Gadd VL, Skoien R, Powell EE, Fagan KJ, Winterford C, Horsfall L, et al. The portal inflammatory infiltrate and ductular reaction in human nonalcoholic fatty liver disease. Hepatology. 2014 Apr 1;59(4):1393–405. [PubMed: 24254368]
28. Williams MJ, Clouston AD, Forbes SJ. Links between hepatic fibrosis, ductular reaction, and progenitor cell expansion. Vol. 146, Gastroenterology. W.B. Saunders; 2014. p. 349–56. [PubMed: 24315991]
29. Thabut D, Shah V. Intrahepatic angiogenesis and sinusoidal remodeling in chronic liver disease: New targets for the treatment of portal hypertension? Vol. 53, Journal of Hepatology. Elsevier B.V.; 2010. p. 976–80. [PubMed: 20800926]
30. Fernández M, Semela D, Bruix J, Colle I, Pinzani M, Bosch J. Angiogenesis in liver disease. Vol. 50, Journal of Hepatology. J Hepatol; 2009. p. 604–20. [PubMed: 19157625]
31. Rama N, Dubrac A, Mathivet T, NíChárthaigh RA, Genet G, Cristofaro B, et al. Slit2 signaling through Robo1 and Robo2 is required for retinal neovascularization. Nat Med. 2015 May 1;21(5):483–91. [PubMed: 25894826]
32. Guo SW, Zheng Y, Lu Y, Liu X, Geng JG. Slit2 overexpression results in increased microvessel density and lesion size in mice with induced endometriosis. ReprodSci. 2013 Mar;20(3):285–98.
33. Taura K, De Minicis S, Seki E, Hatano E, Iwaisako K, Osterreicher CH, et al. Hepatic Stellate Cells Secrete Angiopoietin 1 That Induces Angiogenesis in Liver Fibrosis. Gastroenterology. 2008;135(5):1729–38. [PubMed: 18823985]
34. Lee JS, Kim JH. The role of activated hepatic stellate cells in liver fibrosis, portal hypertension and cancer angiogenesis. Vol. 13, The Korean journal of hepatology. 2007. p. 309–19. [PubMed: 17898548]
35. Franchitto A, Onori P, Renzi A, Carpino G, Mancinelli R, Alvaro D, et al. Expression of vascular endothelial growth factors and their receptors by hepatic progenitor cells in human liver diseases. HepatobiliarySurgNutr. 2013;2(2):68–77.
36. Rodrigo-Torres D, Affò S, Coll M, Morales-Ibanez O, Millán C, Blaya D, et al. The biliary epithelium gives rise to liver progenitor cells. Hepatology. 2014 Oct 1;60(4):1367–77. [PubMed: 24700364]
37. Walter W, Sánchez-Cabo F, Ricote M. GOplot: An R package for visually combining expression data with functional analysis. Bioinformatics. 2015 Feb 6;31(17):2912–4. [PubMed: 25964631]

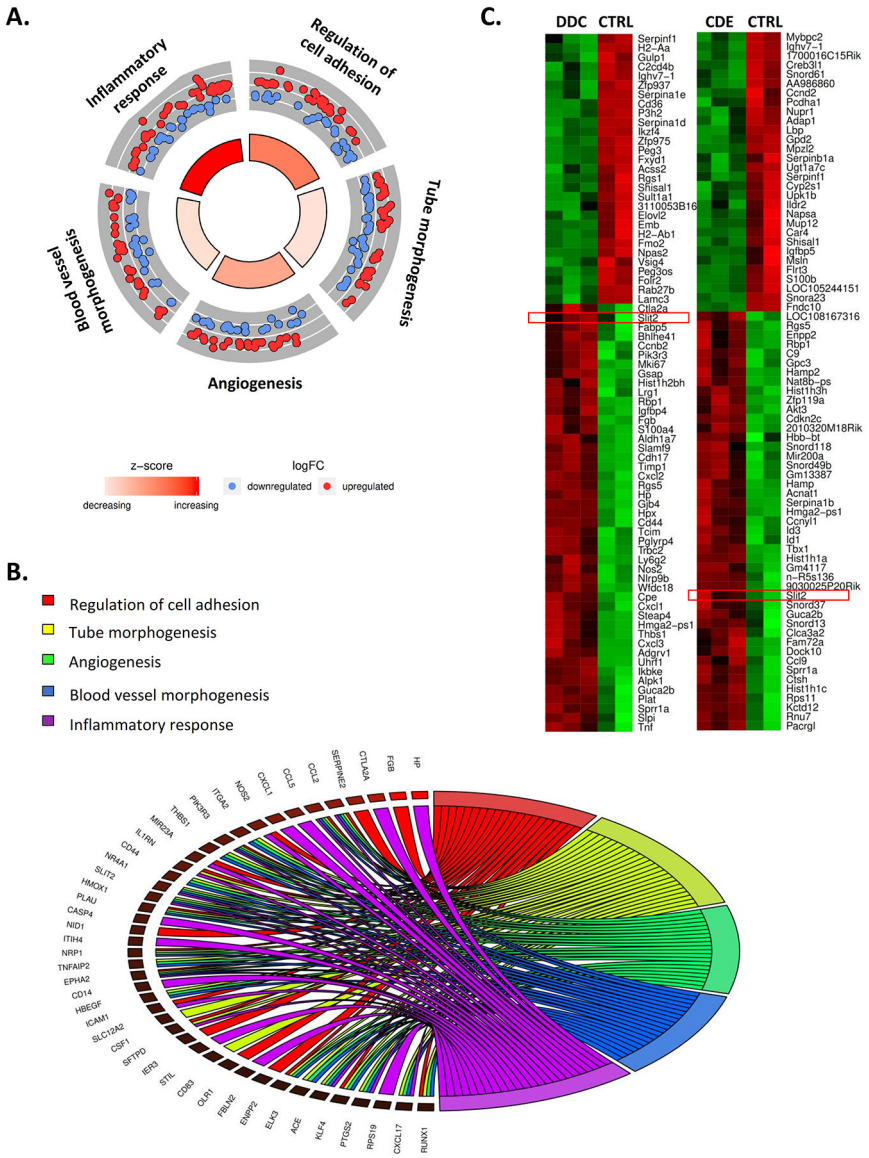

Figure 1. Gene expression and gene ontology (GO) analysis of a transcriptomic dataset derived from ductular reaction cells isolated from HNF1βCreER^{YFP} and control mice.

(A) GO circle plot indicating the top 5 enriched biological processes related to ductular reaction cells of 3,5-diethoxycarbonyl-1,4-dihydro-collidin (DDC) and choline-deficient, ethionine-supplemented diet (CDE) models. The outer ring illustrates the expression sign (blue, down-regulated and red, up-regulated) of the genes included in each GO term. The color intensity of the inner ring shows the significance measured by the z-score for each category. (B) GOChord plot showing genes linked to their assigned GO terms. (C) Heat map displaying the top 75 significantly deregulated genes in YFP^{+} cells isolated from mice receiving DDC or CDE diets for 3 weeks compared to YFP^{+} cells of the control mice.

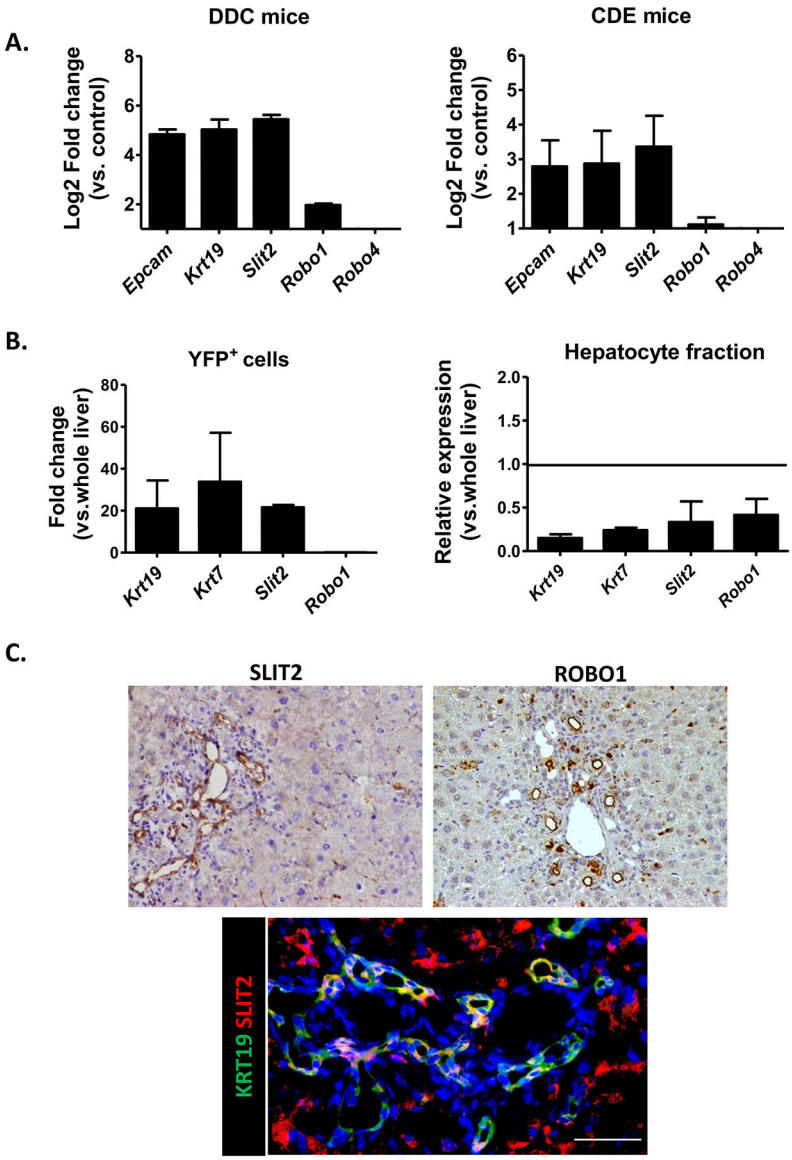

Figure 2. Gene and protein expression of Slit2-Robo1 signaling in mouse models involving ductular reaction proliferation.

(A) Gene expression analysis by qPCR of *Slit2, Robo1, Robo4* and DR markers (*Krt19* and *Epcam*) in whole liver tissue isolated from mice receiving a 3,5-diethoxycarbonyl-1,4-dihydro-collidin (DDC) (n=5) and choline-deficient, ethionine-supplemented diet (CDE) for 3 weeks (n=5). Expression values are represented as Log2 Fold change versus control mice. (B) Levels of gene expression measured by qPCR of key DR markers (*Epcam* and *Krt19*) and *Slit2* and its receptor *Robo1* in YFP+ cells and hepatocyte fraction from livers of mice receiving DDC for 3 weeks. Expression values are represented as fold change versus the expression in whole liver tissue. (C) Representative images at 10x of SLIT2 and ROBO1 immunohistochemistry in liver tissues of a mouse receiving DDC for 3 weeks show the expression of SLIT2 by DR cells and ROBO1 expression restricted to new vessels. Immunofluorescence of KRT19 (green) and SLIT2 (red) confirms co-localization of SLIT2

within the DR. Nuclei counterstaining was performed with DAPI (blue). Scale bar = 100μm. Data presented as mean ± SEM. *p<0.05, **P<0.01 and ***p<0.001.

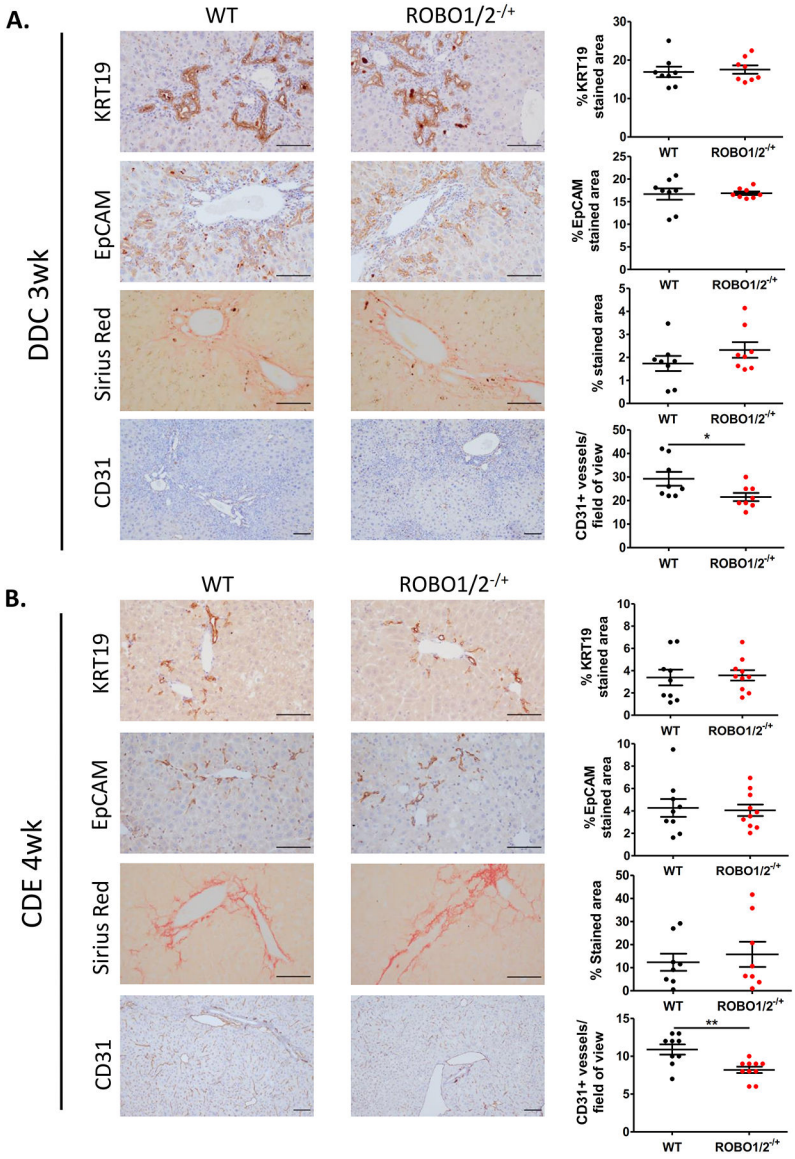

Figure 3. Slit2-Robo1 signaling mediates angiogenesis in both DDC and CDE mouse models.

Representative immunohistochemical staining of KRT19, EPCAM, Sirius Red and CD31 staining in ROBO1/2$^{-/+}$ and WT mice receiving (A) DDC diet for 3 weeks (n=8 in both groups) or (B) CDE diet for 4 weeks (n=9 in WT group, n=10 in ROBO1/2$^{-/+}$ group). In both injury models, DR/progenitor cell expansion and fibrogenesis were evaluated by quantification of positive staining areas for KRT19/EPCAM and Sirius Red, respectively, measured by ImageJ Software. Neo-angiogenesis was quantified by counting the number of CD31 positive vessels surrounding the peri-portal areas/field of view. Scale bars = 100μm. Data is presented as mean ± SEM. Groups were compared by *t-test* analysis. *p<0.05 and **P<0.01.

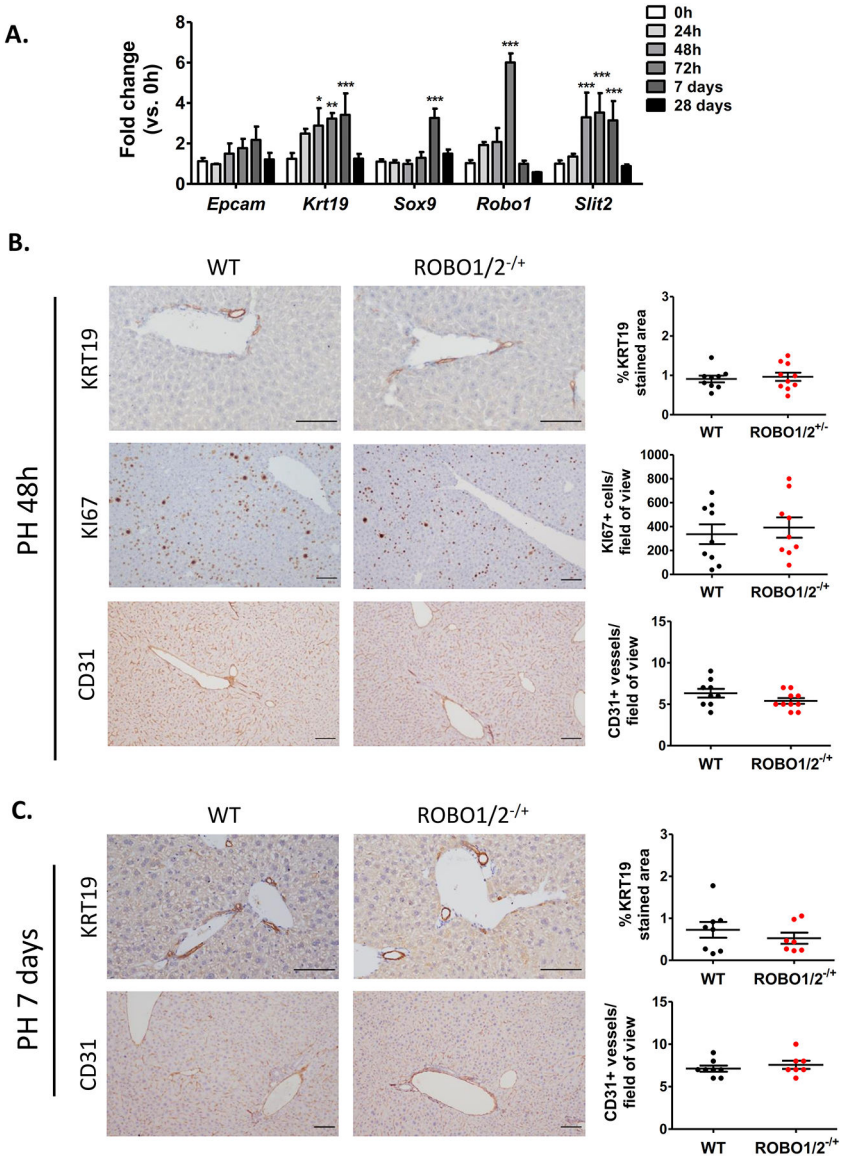

Figure 4. Slit2-Robo1 signaling does not participate in partial hepatectomy regeneration.

(A) Gene expression analysis of liver progenitor cell markers (*Krt19*, *Epcam* and *Sox9*), *Slit2* and *Robo1* in mouse livers at early (24, 48 and 72 hours after surgery) and late (day 7 and day 28) time points after two thirds partial hepatectomy in WT mice (n= 3 to 5 mice per group). Fold change is represented as expression at each time point versus expression at day 0. Grouped analysis was compared by two-way ANOVA with Bonferroni post-test correction. *p<0.05, **p<0.01, ***p<0.001. (B) Two thirds partial hepatectomy was evaluated in WT and ROBO1/2$^{-/+}$ mice (n= 9 in WT group and n=10 in ROBO1/2$^{-/+}$ group), being sacrificed at 48 hours after the surgery. (C) Two thirds partial hepatectomy was performed in WT and ROBO1/2$^{-/+}$ mice (n= 8 in WT group and n=7 in ROBO1/2$^{-/+}$ group), and animals were sacrificed at day 7 after the surgery. (B) Representative images of cell proliferation at 48 hours evaluated by KI67 staining. (B-C) Representative immunohistochemical staining for CD31 and KRT19 in livers after 48 hours

and 7 days after partial hepatectomy. DR expansion and cell proliferation were measured by the quantification of positive staining for KRT19 and KI67, respectively, by ImageJ Software. New vessel formation was evaluated by counting $CD31^+$ vessels/field of view. Scale bars = 100μm. Data presented as mean ± SEM. Groups were compared by *t-test* analysis.

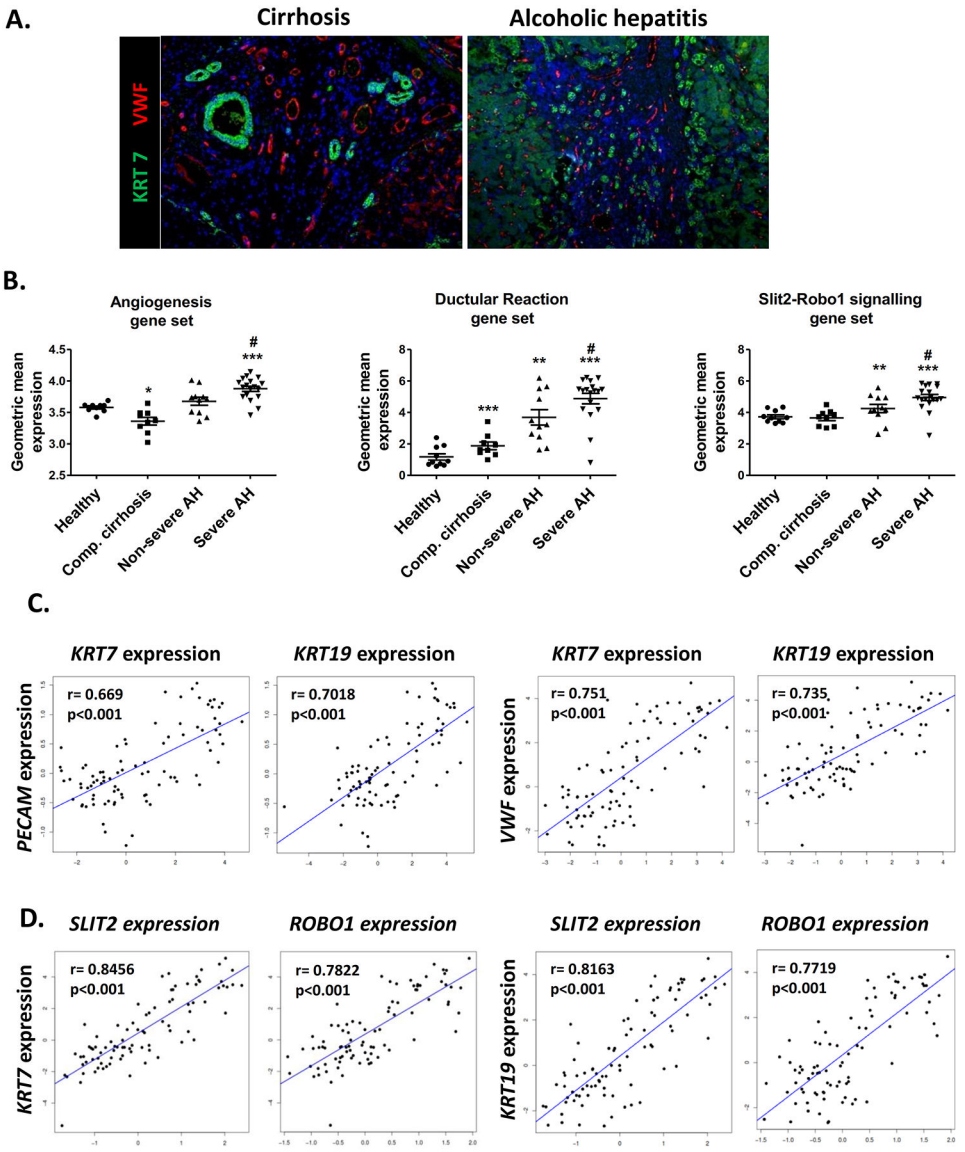

Figure 5. Expression profile of Slit2-Robo1 signaling, angiogenesis and ductular reaction gene sets along ARLD progression.

(A) Representative double immunostaining for KRT7 and VWF in paraffin-embedded sections of liver tissues from cirrhotic and AH patients showing neo-angiogenesis surrounding the peri-portal areas where DR expands. Nuclei counterstaining was performed with DAPI (blue). (B) Hepatic gene expression levels of angiogenesis, DR gene sets and Slit2-Robo1 signaling in patients with compensated cirrhosis, patients with non-severe AH (MELD<21), severe AH (MELD<21) and healthy individuals, and (C) Correlations of hepatic gene expression of DR markers (*KRT7* and *KRT19*) with angiogenesis markers (*PECAM* and *VWF*) and with *SLIT2* and *ROBO1* expression (D). The liver transcriptomic data was obtained from a cohort of patients encompassing the ARLD spectrum: patients with early alcoholic steatohepatitis (ASH) were non-obese individuals with high alcohol intake, mild elevation of transaminases and histologic criteria of steatohepatitis (ASH, n = 12), patients with histologically confirmed AH by biopsy (AH non-severe, n = 18), liver

explants from patients with AH who underwent early transplantation (severe AH, n = 11) were compared to non-diseased human livers (healthy, n=10), patients with non-cirrhotic HCV infection (compensated cirrhosis, n = 10), patients with non-alcoholic fatty liver disease (NAFLD) according to Keiner's Criteria and without alcohol abuse (n = 9) and patients with compensated HCV-related cirrhosis (n = 9). Data presented as mean ± SEM. Gene expression was analyzed vs. healthy (*$p<0.05$, **$p<0.01$ and ***$p<0.001$) and vs. non-severe AH ($^{\#}p<0.05$).

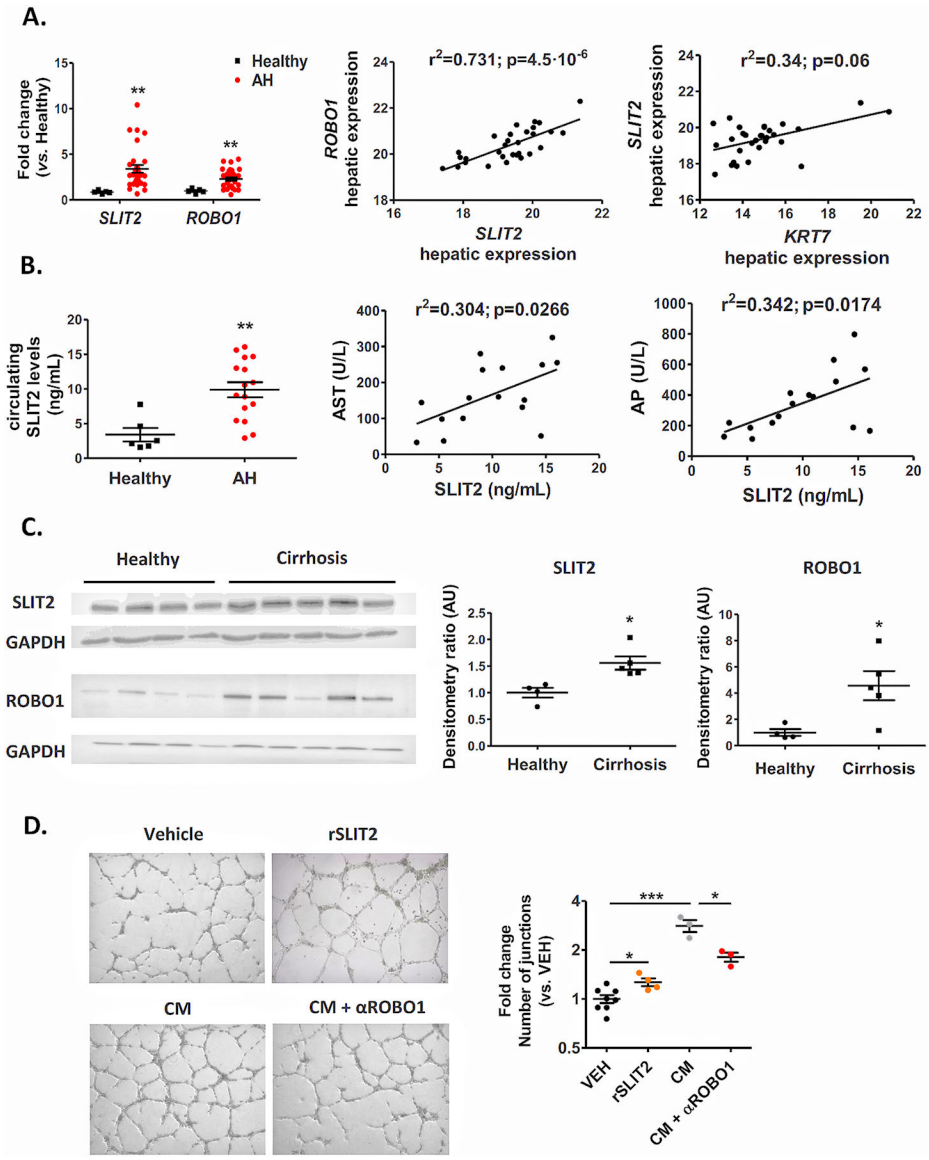

Figure 6. Alcoholic hepatitis patients display increased hepatic expression of Slit2-Robo1 signaling and enhanced SLIT2 serum levels. Ductular reaction cells from cirrhotic liver secrete SLIT2 and mediate angiogenesis.

(A) *SLIT2* and *ROBO1* expression levels measured by qPCR in liver biopsies of AH (n=29) and healthy individuals (n=5). Correlation of hepatic gene expression assessed by qPCR of *SLIT2* with *ROBO1* and *KRT7* in patients with AH (n=29). The regression coefficient (r^2) and p value are indicated. (B) Serum levels of SLIT2 measured in healthy controls (n=6) and AH patients (n=16) by ELISA. Data presented as mean ± SEM. *p<0.05, **p<0.01. (C) Protein expression analysis by Western Blot of SLIT2 and ROBO1 in livers from cirrhotic (n=4) and healthy subjects (n=4). Quantification of protein levels was performed by densitometry analysis. As a loading control, an antibody against GAPDH was used. (D) Tubulogenic assay performed by exposing HUVECs to organoid basal medium (n=8 technical replicates), human recombinant Slit2 (2ng/mL) (n=4 technical replicates), conditioned medium of 3 cirrhotic organoids (n=3 organoids generated from 3 different

cirrhotic liver tissue explants) and conditioned medium plus αROBO1 antibody for 12 hours. Angiogenic capacity was evaluated by counting the number of junctions formed by using Angiogenesis Analyzer tool of ImageJ Software. Data is representative from three independent experiments, represented as the mean fold change ± SEM versus organoid basal medium group average. Groups were compared by t-test analysis. *$p<0.05$, ***$p<0.001$.